Theoretical prediction of the optimal conditions for observing the stereodynamical vector properties of the $C(^3P) + OH\ (X^2\Pi) \rightarrow CO(X^1\Sigma^+) + H(^2S)$ reaction*

Wang Yuan-Peng(王远鹏)[a], Zhao Mei-Yu(赵美玉)[b], Yao Shun-Huai(姚舜怀)[c], Song Peng(宋 朋)[a]†, and Ma Feng-Cai(马凤才)[a]‡

[a] *Department of Physics, Liaoning University, Shenyang* 110036, *China*
[b] *Institute of Theoretical Simulation Chemistry, Academy of Fundamental and Interdisciplinary Sciences, Harbin Institute of Technology, Harbin* 150080, *China*
[c] *School of Physics, Peking University, Beijing* 100871, *China*

(Received 21 February 2013; revised manuscript received 9 May 2013)

The best optimal initial reactant state and collision energy for observing the stereodynamical vector properties of the title reaction in the ground electronic state X^2A' potential energy surface (PES) [Zanchet *et al.* 2006 *J. Phys. Chem. A* **110** 12017] are theoretically predicted using the quasi-classical trajectory (QCT) method for the first time. The calculated results reveal that the smallest value of the rotational quantum number j, larger vibrational quantum number v, and the lower strength of collision energy should be selected for offering the most obvious picture about the stereodynamical vector properties. Polarization-dependent differential cross sections and the angular momentum alignment distribution, $P(\theta_r)$ and $P(\Phi_r)$ in the center-of-mass frame, are obtained to gain an insight into the alignment and orientation of the product molecules. The rotational angular momentum vector j' of CO is aligned to be perpendicular to reagent relative velocity k. The product polarizations align along the y axis, pointing to the positive direction of the y axis. A new method is developed to investigate massive reactions with various initial states and to further study the vector properties of the fundamental reactions in detail.

Keywords: quasi-classical trajectory, initial states, stereodynamics, polarization, collision energy

PACS: 82.20.Fd, 71.15.Pd **DOI:** 10.1088/1674-1056/22/12/128201

1. Introduction

The reaction between open-shell C atoms and OH radicals, which is known as one of the most important and typical hydroxyl radiation reactions, has gained increasing attention in the fields of astrophysics, nebula, and atmospheric chemistry.[1,2] In particular, the title reaction is included in nebulas, which mainly include carbon-, nitrogen- and oxygen-containing species. Though the HCO radical has been widely studied for its photo-dissociation spectrum, the COH is considered as a meta-stable species and has never been investigated. It should be noted that the C + OH reaction presents interesting phenomena for combustion in the high temperature range.[3] Despite its short lifetime, the OH radical reacts with a lot of compounds and acts as a cleaner of the atmosphere, because it can finish the transformation of the active species into inactive ones.[4] Unfortunately, the difficulty in performing any experiments on some conditions such as low temperature keeps us away from investigating this class of reaction in the laboratory.[5,6] Besides, such reactions usually involve potential energy surfaces (PESs) with deep potential wells, and for such systems containing two heavy atoms, many channels have to be considered to obtain converged results.[4] So when we are trying to explain it, darkness still covers the nature of this reaction: the lack of experimental rate constant and the difficulty in overcoming theoretical study's barriers. Because of the limited resource, only some theoretical predictions could be done.[1,7]

As is well known, Graff firstly gave some meaningful results based on the adiabatic capture-infinite order sudden approximation and obtained an upper limit of 10^{-12} $cm^3 \cdot s^{-1}$ for the rate constant.[8] Most importantly, to the best of our knowledge, a global potential energy surface (PES) for the $C(^3P) + OH(X^2\Pi) \rightarrow CO(X^1\Sigma^+) + H(^2S)$ reaction in the ground X^2A' state by using the high level *ab initio* calculations have been reported by Zanchet *et al.*[9] From then on, numerous theoretical studies, by using quantum mechanical (QM) and quasi-classical trajectory (QCT) methods, were performed to explore the reaction dynamics of the title reaction based on this PES.[10–15] For example, Zanchet *et al.*[10] studied the relation of integral cross section to collision energy and the temperature-independent thermal rate coefficients at

*Project supported by the Program of Shenyang Key Laboratory of Optoelectronic Materials and Technology, China (Grant No. F12-254-1-00), the National Natural Science Foundation of China (Grant No. 11274149), and the Natural Science Foundation of Liaoning Province, China (Grant No. 20111035).

†Corresponding author. E-mail: songpeng@lnu.edu.cn
‡Corresponding author. E-mail: fcma@lnu.edu.cn

© 2013 Chinese Physical Society and IOP Publishing Ltd

high temperatures by employing the QCT method. Also the QCT calculations were performed to obtain differential cross sections (DCSs) and product energy distributions in a wide range of collision energies.[10] The influences of the reagent diatom rovibrational excitation on these quantities were explored, and the results demonstrated that reaction probabilities were weakly dependent on the initial rotational quantum state of the OH, and the v and j state-selected rate coefficients were practically insensitive to temperature, except for those in the low temperature region. These results were found to be accordant with real wave packet (RWP) calculations, which indicated that QCT results were quite acceptable.[15] At the same time, Lin *et al.*[11] calculated the exact reaction probability at the total angular momentum $J = 0$, using the wave packet method, for the first time. Gray *et al.*[12] employed the capture model to obtain good simulations of the $J > 0$ reaction probability, the integral cross section and rate constant, due to the large exothermic and barrierless nature of the title reaction.

However, only understanding the scalar dynamics properties is less than enough to state the nature of the title reaction. Stereodynamics of chemical reactions cover the relative velocities of the reagent and product (k/k') and the product rotational angular momentum (j), which not only contain information about the translation and rotational energy discussed by Zanchet *et al.*,[10,14] but also provide us with a clear view about the polarization of the products.[2,16–18] In detail, stereodynamics includes the information about the angular distributions of $P(\theta_r)$ and $P(\Phi_r)$, as well as the polarization-dependent differential cross sections (PDDCSs) in the sense of the product polarization within the center-of-mass (CM) frame.[19] So, the vector properties, which provide valuable information about chemical reaction stereo-dynamics, should be further studied. And the possible correlations among them for a thorough picture could be formed as well.[2,3,16,20,21] Up to now, the product rotational polarization of the title reaction has been investigated in a wide range of collision energies (1 kcal/mol–46 kcal/mol).[19] And the product rotational polarizations under different initial conditions ($E_{\rm col}$ = 1 kcal/mol–46 kcal/mol, $v = 0$–2, $j = 0$–10) were found to be qualitatively similar to the product rotational angular momentum mainly aligned to be perpendicular to the reaction plane.[3] As is well known, the polarization degree is significantly influenced by initial conditions. But the optimal initial conditions for offering the most obvious images of the stereodynamical vector properties are still unknown.

For this purpose, firstly, the $P(\theta_r)$ and $P(\Phi_r)$ distributions in different initial states of $v = 0$–2, $j = 0$–5 and with different collision energies are obtained. Based on these results, the detailed analysis and comparison can be performed to provide the trend of distributions under the initial conditions, and therefore the optimal initial conditions are safely obtained.

2. Computational aspects

2.1. Quasi-classical trajectory calculations

All the calculations on the C + OH reaction in this paper are performed using the QCT code written by Han and coworkers,[17,22–27] and the QCT method used here is similar to that described therein. We summarize here only the most relevant details to the present study. Classical Hamilton's equations are numerically integrated in three dimensions. By setting the initial rotational quantum number $j = 0$–5 and initial vibration number $v = 0$–2 of OH, a batch of 5×10^4 trajectories started from 20-Å initial CM separation and then run with the appropriate value of the maximum impact parameter which varied from 5.6 Å to 3.2 Å as energy increases. The impact parameters were pre-optimized before running the trajectories at each collision energy. The collision energies in this paper are intentionally chosen for the convenience of comparison with the results of relevant studies. The Hamilton's motion equation is solved by the symplectic integration method in integration steps of 0.1 fs, which guarantees the conservations of the total energy and total angular momentum.

2.2. Product rotational polarization

The vector correlation $(k$–$j')$ is expanded in a series of Legendre polynomials and the distribution $P(\theta_r)$ can be written as[18,28,29]

$$P(\theta_r) = \frac{1}{2}\sum_k [k] a_0^k \mathrm{P}_k(\cos\theta_r)^*, \tag{1}$$

where

$$a_0^k = \langle \mathrm{P}_k(\cos\theta_r)\rangle. \tag{2}$$

The expanding coefficients (polarization parameters) are called the orientation (k is odd) or alignment (k is even) parameters.

The dihedral angle distribution function $P(\Phi_r)$ describing the k–k'–j' correlations can be expanded in a series of Fourier series as[30–32]

$$P(\phi_r) = \frac{1}{2\pi}\left(1 + \sum_{\text{even},n\geq 2} a_n \cos n\Phi_r + \sum_{\text{odd},n\geq 1} b_n \sin n\Phi_r\right), \tag{3}$$

where

$$a_n = 2\langle \cos n\Phi_r\rangle, \tag{4}$$

$$b_n = 2\langle \sin n\Phi_r\rangle. \tag{5}$$

Here, θ_r and Φ_r are the polar angles that determine the direction of product angular momentum j' as shown in Fig. 1.

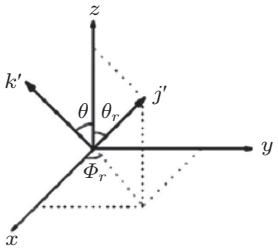


Fig. 1. Center-of-mass coordinate system used to describe the $\boldsymbol{k}'$ and $\boldsymbol{j}'$ correlations.

3. Results and discussion

3.1. Distributions of $P(\theta_r)$ in different initial states

By setting the initial rotational quantum number $j = 0$ and initial vibrational quantum number $v = 0$–2 of OH, the calculated distributions of $P(\theta_r)$ for CO at different collision energies are presented in the left panel of Fig. 2. From the plots, we can conclude that the product is strongly polarized, which is in accordance with the results reported previously.[19] The product channel in the ground electronic state X^2A' illustrates symmetric distributions peaked at $\theta_r = 90°$ indicating that the product rotational angular momentum vector tends to strongly align in the direction perpendicular to the scattering plane. In addition, as collision energy increases there is an enhancement in each of the calculated $P(\theta_r)$ distributions, which means the alignment of the product molecule becomes stronger at high energies.

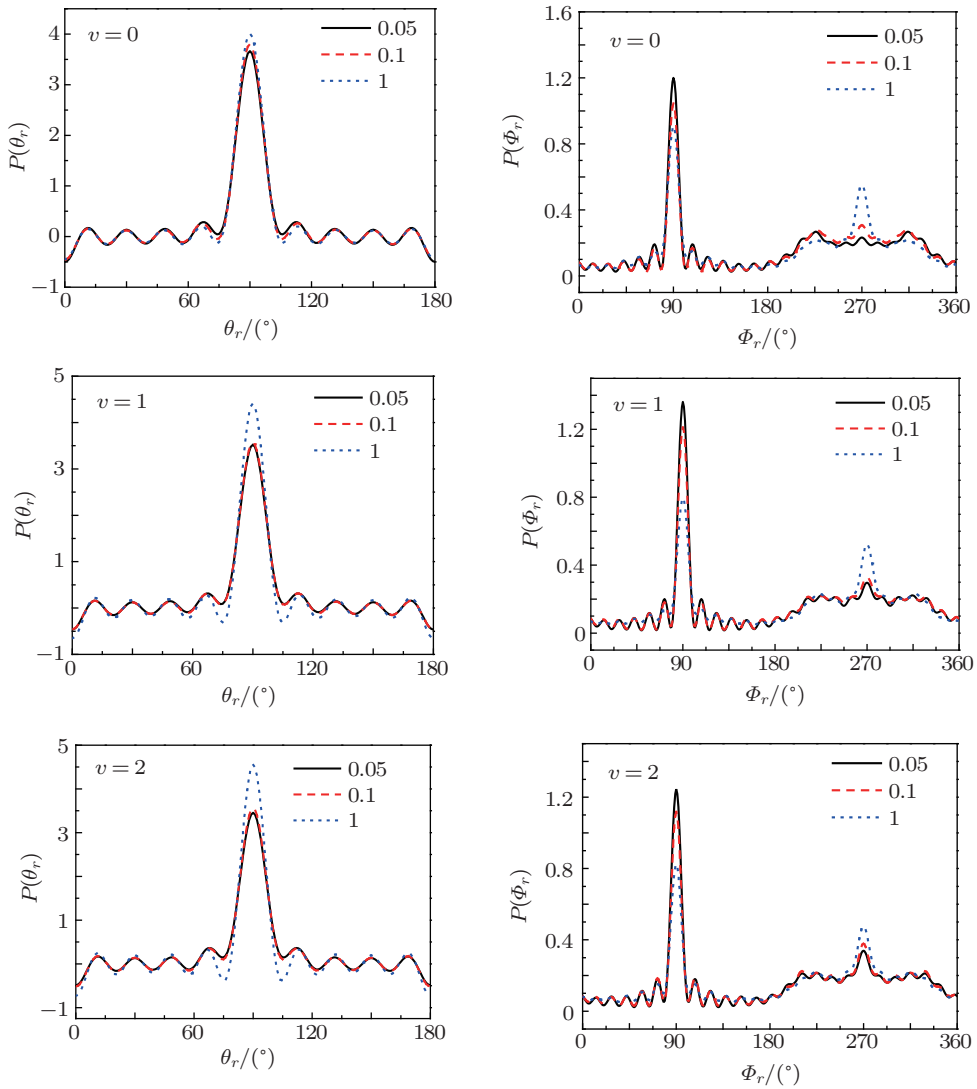


Fig. 2. (color online) Distributions of $P(\theta_r)$ and $P(\Phi_r)$ for the CO product from the reaction C + OH $(v, j) \rightarrow$ CO (v', j') + H at the collision energies of 0.05, 0.1, and 1 eV with $j = 0$ and $v = 0$–2.

In order to investigate the detailed stereo-dynamic properties of the title reaction, namely, the influence of the initial quantum number on $P(\theta_r)$ distribution, comparisons among the peak values of $P(\theta_r)$ at $\theta_r = 90°$ with different initial states at different collision energies are performed. The results are presented in Fig. 3. As can be seen from Fig. 3, the peak val-

ues of $P(\theta_r)$ each have a general decreasing tendency with the increase of quantum number j, regardless of the collision energy or the quantum vibrational number v. It should be noted that there are some exceptions. But all of these exceptions cannot change or affect the decreasing tendency of $P(\theta_r)$ peak value with the increase of j. So the characteristic of the k–j' vector correlation of the title reaction can be more easily observed when the quantity of j is small. On the other hand, the change tendency of the $P(\theta_r)$ peak values with the quantum number v looks more complicated, which should be described separately in detail. As can be seen from Fig. 3, when j is relatively large ($j = 3$–5), the increasing of the vibrational quantum number v makes the polarization of the product stronger in the direction perpendicular to the scattering plane. When the rotational quantum number is small ($j = 0$–2), the peak values of $P(\theta_r)$ vary with vibrational number and collision energy range, which can be described below in two cases. For the first case, the collision energy is large enough (high collision energy range, 0.5 eV$\sim$ 1 eV), the peak values of $P(\theta_r)$ decrease with higher rotational excitation of reactant. For the second case, the collision energy is in the lower strength (low collision energy range, 0.05 eV$\sim$ 0.1 eV), the difference in $P(\theta_r)$ peak value between different values of initial v is slight.

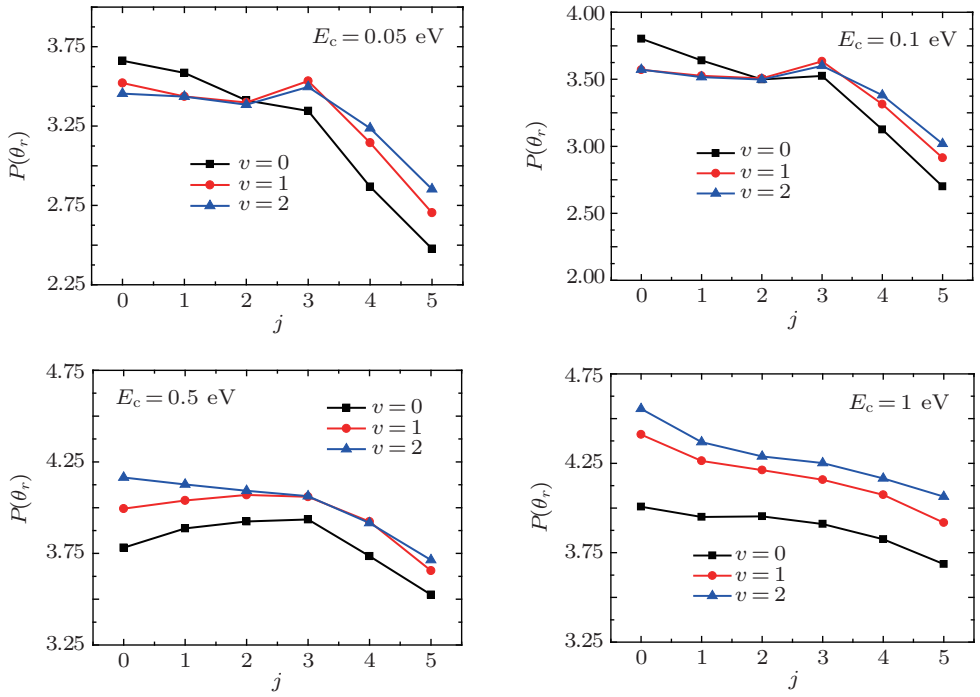


Fig. 3. (color online) Comparisons among the peak values of $P(\theta_r)$ at $\theta_r = 90^\circ$ of different initial states at different collision energies.

From all the analysis mentioned above, the complicated tendency of how the maximum $P(\theta_r)$ distribution varies with v still leaves us uncertainty to obtain an accurate quantity of v for obtaining the obvious characteristics of the vector properties of the title reaction. And to choose the vibrational quantum number in theoretical predictions, further investigation is needed.

3.2. Distributions of $P(\Phi_r)$ in different initial states

Because Φ_r determines the dihedral angle between the planes consisting of k–k' and k–j', the $P(\Phi_r)$ distribution describes the k–k'–j' vector correlation and can provide stereodynamical information about both product alignment and product orientation.[19] Similar to the previous studies, as can be seen from the right panel of Fig. 2, the peaks of $P(\Phi_r)$ appear at $\Phi_r = 90^\circ$ (large peak) and $\Phi_r = 270^\circ$ (small peak), which shows that the product tends to align along the direction of the y axis, and orient along the positive direction of the y axis. In other words, the product molecules prefer a counterclockwise rotation in the plane parallel to the scattering plane. In addition, a rather isotropic behavior with respect to Φ_r (no obvious peaks appear) at larger Φ_r range ($180^\circ \sim 360^\circ$) disappears with the increase of collision energy. The polarization behaviors observed above can be explicitly traced to the insertion reaction mechanism that largely dominates the dynamics on this attractive potential energy surface,[2] which is in accordance with the formation of long-lived intermediate complex HCO at high collision energy.[10]

For our main purpose of this paper, the different initial rotational and vibrational quantum numbers of OH are considered and the calculated maximum $P(\Phi_r)$ distribution results are presented in Fig. 4, by setting $j = 0$–5 and $v = 0$–2 at different collision energies. Obviously, as can be seen from Fig. 4, the maximum $P(\Phi_r)$ distributions decrease with the increase of the initial rotational angular momentum vector j, especially in the low collision energy range. This is in accordance with that of $P(\theta_r)$, and indicates that a small value of the quantum number j should be selected, again. Unlike the $P(\theta_r)$, the influence of setting different values of initial v on the maximum $P(\Phi_r)$ distribution behaves simply. From Fig. 4, in the low collision energy range, larger vibrational quantum number is of benefit to the observation of stereodynamical information about both product alignment and product orientation. With the increase of the collision energy, the undulation of the maximum $P(\Phi_r)$ distributions makes it reasonable to conclude that it is almost insensitive to the initial setting of v, which can be obviously seen from the result at the collision energy 1 eV in Fig. 4. Furthermore, detailed analysis of Fig. 4 also provides that 0.05 eV is the beginning of the collision energy that the change of $P(\Phi_r)$ distribution dependent on quantum number v could be ignored.

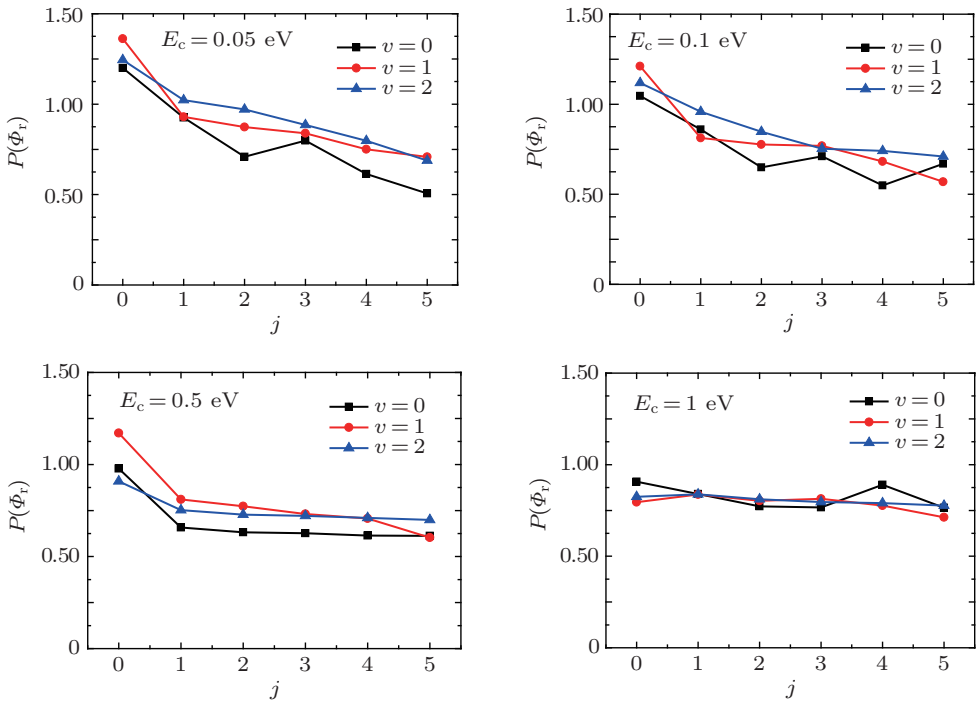


Fig. 4. (color online) Comparisons among the peak values of $P(\Phi_r)$ at $\theta_r = 270°$ of different initial states at different collision energies.

Collision energy, as another determinative factor for observing the vector properties of the title reaction, has been discussed above to some degree. But until now, it is still unknown what collision energy is the best for providing the stereodynamical information in the cases of product alignment and product orientation. Further investigation into the variation of the peak values of $P(\Phi_r)$ at $\theta_r = 270°$ with different collision energies indicates that the conclusion is not hard to reach. From Fig. 5, it can be easily found that the vector characteristic of $P(\Phi_r)$ distribution decreases with collision energy increasing, except for $P(\Phi_r)$ at $v = 0$ and $j = 1$–5. In the low collision energy range, the larger the vibrational quantum number v, the slower the descending tendency of the maximum $P(\Phi_r)$ distributions is. Note that in the higher collision energy range, the maximum $P(\Phi_r)$ distributions tend to be similar, with relatively small values (see $v = 2$ in Fig. 5). So, if the $P(\Phi_r)$ distribution of the title reaction is expected to be observed obviously, the low collision energy should be selected.

Finally, considering what has been stated above, it is safe to conclude that the specific initial states of OH and the appropriate collision energy, which can offer the most obvious images of the stereodynamical vector properties of the title reaction, are the smallest rotational quantum number j, larger vibrational quantum number v, and the lower strength of collision energy, which should be selected.

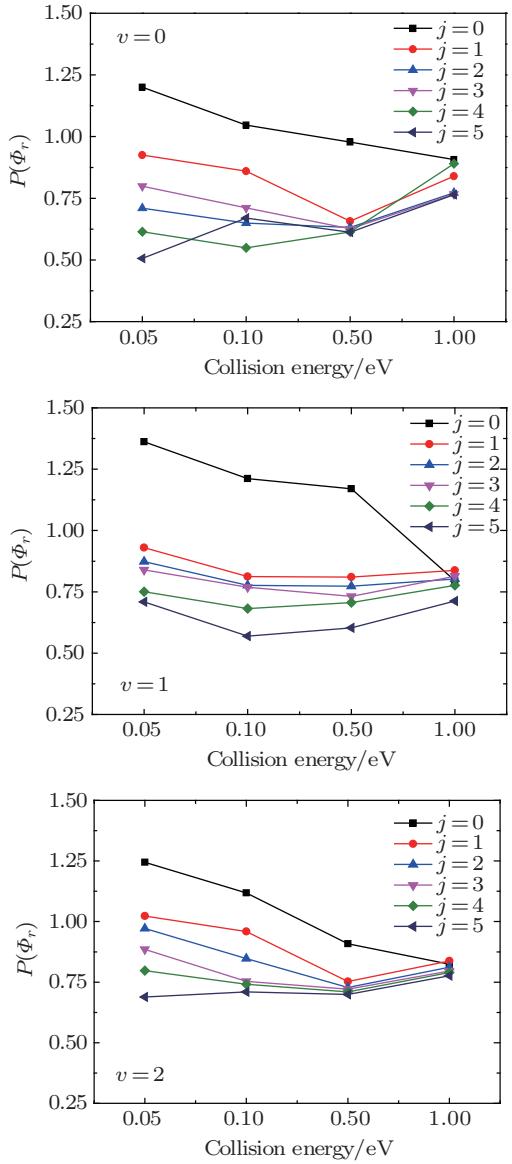


Fig. 5. (color online) Comparisons among the peak values of $P(\Phi_r)$ at $\theta_r = 270°$ of different collision energies by setting the different initial states.

4. Conclusions

In summary, we perform QCT calculations to investigate the detailed stereodynamics properties for the reaction $C(^3P) + OH(X^2\Pi) \rightarrow CO(X^1\Sigma^+) + H(^2S)$ using the *ab initio* PES recently developed by Zanchet *et al.* The results reveal that the rotational angular momentum vector j' of CO is preferentially aligned in the direction perpendicular to k, and the product polarization, depicted by the $P(\Phi_r)$ distributions, mainly aligned along the y axis, pointing to the positive direction of the y axis. Most importantly, the theoretical predictions of the optimal initial reactant states and collision energy for offering the most obvious images of the stereodynamical vector properties of the title reaction are made for the first time. As a conclusion, the smallest value of the rotational quantum number j, larger vibrational quantum number v, and the lower strength of collision energy should be selected.

References

[1] Chu T S, Zhang Y and Han K L 2006 *Int. Rev. Phys. Chem.* **25** 201
[2] Chu T S 2010 *J. Comput. Chem.* **31** 1385
[3] Ding Y J and Shi Y 2011 *Comput. Theor. Chem.* **963** 306
[4] Wei Q 2012 *J. Theor. Comput. Chem.* **11** 811
[5] Casavecchia P 2000 *Rep. Prog. Phys.* **63** 55
[6] Carty D, Goddard A, Kohler S P K, Sims I R and Smith I W M 2006 *J. Phys. Chem. A* **110** 3101
[7] Zhang W Q, Cong S L, Zhang C H, Xu X S and Chen M D 2009 *J. Phys. Chem. A* **113** 4192
[8] Graff M M 1989 *Astrophys. J.* **339** 239
[9] Zanchet A, Bussery-Honvault B and Honvault P 2006 *J. Phys. Chem. A* **110** 12017
[10] Zanchet A, Halvick P, Rayez J C, Bussery-Honvault B and Honvault P 2007 *J Chem. Phys.* **126** 184308
[11] Lin S Y, Guo H and Honvault P 2008 *Chem. Phys. Lett.* **453** 140
[12] Gray S K, Goldfield E M, Schatz G C and Balint-Kurti G G 1999 *Phys. Chem. Chem. Phys.* **1** 1141
[13] Bussery-Honvault B, Dayou F and Zanchet A 2008 *J. Chem. Phys.* **129** 234302
[14] Zanchet A, Halvick P, Bussery-Honvault B and Honvault P 2008 *J. Chem. Phys.* **128** 204301
[15] Bulut N, Zanchet A, Honvault P, Bussery-Honvault B and Banares L 2009 *J. Chem. Phys.* **130** 194303
[16] Han K L, He G Z and Lou N Q 1993 *Chin. Chem. Lett.* **4** 517
[17] Li B and Han K L 2009 *J. Phys. Chem. A* **113** 10189
[18] Han K L, He G Z and Lou N Q 1996 *J. Chem. Phys.* **105** 8699
[19] Song P, Zhu Y H, Liu J Y and Ma F C 2010 *J. Theor. Comput. Chem.* **9** 935
[20] Zhang W Q, Li Y Z, Xu X S and Chen M D 2010 *Chem. Phys.* **367** 115
[21] Duan L H, Zhang W Q, Xu X S, Cong S L and Chen M D 2009 *Mol. Phys.* **107** 2579
[22] Zhang C H, Zhang W Q and Chen M D 2009 *J. Theor. Comput. Chem.* **8** 403
[23] Li H, Zheng B, Yin J Q and Meng Q T 2011 *Chin. Phys. B* **20** 123401
[24] Bai M M, Ge M H, Yang H and Zheng Y J 2012 *Chin. Phys. B* **21** 123401
[25] Xu Z H, Zong F J and Han B R 2012 *Chin. Phys. B* **21** 093103
[26] Guo Y H, Zhang F Y and Ma H Z 2013 *Commn. Comput. Chem.* **1** 99
[27] Yang T G, Yuan J C, Cheng D H and Chen M D 2013 *Commn. Comput. Chem.* **1** 15
[28] Yue X F 2012 *Chin. Phys. B* **21** 073401
[29] Li R J, Han K L, Li F E, Lu R C, He G Z and Lou N Q 1994 *Chem. Phys. Lett.* **220** 281
[30] Wang M L, Han K L and He G Z 1998 *J. Phys. Chem. A* **102** 10204
[31] Chen M D, Han K L and Lou N Q 2003 *J. Chem. Phys.* **118** 4463
[32] Chen M D, Wang M L, Han K L and Ding S L 1999 *Chem. Phys. Lett.* **301** 303